

---

## CONDENSED-MATTER SPECTROSCOPY

---

# Control of Absorption Spectrum of a One-Dimensional Resonant Photonic Crystal

**S. Ya. Vetrov<sup>a</sup>, I. V. Timofeev<sup>b</sup>, and A. Yu. Avdeeva<sup>a</sup>**

<sup>a</sup> Siberian Federal University, Krasnoyarsk, 660074 Russia

<sup>b</sup> Kirensky Institute of Physics, Siberian Branch, Russian Academy of Sciences,  
Akademgorodok, Krasnoyarsk, 660036 Russia

e-mail: avdeeva-anastasiya@yandex.ru

Received February 9, 2010

**Abstract**—The crystal under consideration is a layered structure consisting of alternating layers of two materials, one of which is a resonantly absorbing gas. It is shown that the combination of the dispersion of an atomic gas with the dispersion of a photonic-bandgap structures allows one to efficiently control the transmission spectra of *s*- and *p*-polarized modes in these combined systems. It is found that the spectrum is highly sensitive to the position of the gas resonance frequency with respect to the bandgap edge and to a change in the gas pressure. The transmission, reflection, and absorption spectra of the resonant photonic crystal are studied at an angle of incidence equal to the Brewster angle of a seed photonic crystal. Possible applications of the found particular features of the dispersion of resonant photonic crystals are discussed.

**DOI:** 10.1134/S0030400X10070179

### INTRODUCTION

Photonic crystals are, as a rule, artificial structures whose dielectric permittivity periodically changes in space. Due to the spatial periodicity, the spectra of electromagnetic waves in these structures have a band character, just as a spatially periodic potential is responsible for the band spectrum of electrons. Due to the existence of photonic bandgaps and regions of anomalously increased density of photonic states, photonic crystals are of undoubted interest from the viewpoint of efficient control of laser radiation characteristics [1–3].

Photonic crystalline materials served as a basis for creating new types of waveguides [4, 5], for developing new methods of increasing the efficiency of nonlinear optical processes [6–8], and for discussing ideas on the development of hardware components of optoelectronic industry and information technologies [9].

The spectral properties of photonic crystals can be considerably changed by introducing resonant media (atomic or molecular gases) inside the periodic structure. However, these changes are only manifested in a narrow frequency region near the resonance frequency, as a result of which these photonic crystals are called resonant photonic crystals. The simplest resonant photonic crystals are layered structures consisting of alternating layers of two materials, one of which can be a resonantly absorbing gas. The combination of the resonant dispersion of a gas with the dispersion of a photonic crystal structure leads to qualitative changes in the spectra of photonic crystals, namely, to the appearance of narrow transmission bands in the pho-

tonic bandgap and additional bandgaps in the continuous spectrum. The spectral properties of these resonant photonic crystals were studied in [10, 11] for the normal incidence of radiation on the sample. The angular dependence of the additional transmission spectrum of resonant photonic crystals was studied in [12].

In this study, as distinct from [12], we obtained a significant increase in the transmission coefficient of a resonant photonic crystal due to a change in the structure parameters. In particular, we showed that the transmission spectrum is rather sensitive to variations in the angle of incidence. It was found that an angle of incidence exists at which an additional bandgap appears in the continuous spectrum of a photonic crystal. In addition, we studied the transmission, reflection, and absorption spectra of resonant photonic crystals at an angle of incidence equal to the Brewster angle of a seed photonic crystal.

### EXPRESSIONS FOR TRANSMISSION, REFLECTION, AND ABSORPTION COEFFICIENTS

Let us consider a photonic crystal structure in the form of a finite layered structure with a resonant gas as one of its alternating isotropic layers. This structure (Fig. 1) is characterized by the dielectric permittivities of the layers of the isotropic medium  $\epsilon_1$  and the gas  $\epsilon_2(\omega)$ . The thicknesses of the layers are  $d_1$  and  $d_2$ , and the structure period is  $L = d_1 + d_2$ . In the Lorentz

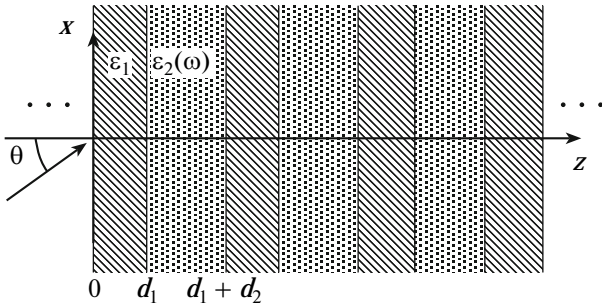


**Fig. 1.** Schematic of periodic layered structure.

approximation, the complex dielectric permittivity of a medium is given by the expression

$$\varepsilon_2(\omega) = 1 + \frac{\omega_p^2}{\omega_0^2 - \omega^2 + i\gamma\omega}, \quad (1)$$

where  $\omega_p^2 = 4\pi Nfe^2/m$ ,  $e$  is the electron charge,  $m$  is the electron mass,  $N$  is the density of resonant atoms,  $f$  is the oscillator strength,  $\gamma$  is the linewidth,  $\omega_0$  is the central frequency of the resonance, and  $\omega$  is the radiation frequency.

We will study the absorption spectrum of *p*-polarized waves propagating in the *xz* plane of a resonant photonic crystal by the transfer-matrix method [13]. For the structure under study, the electric field distribution in the layers has the form

$$E_x(n, t) = [A_n e^{i\alpha_n(z-z_n)} + B_n e^{-i\alpha_n(z-z_n)}] e^{-i\omega t}, \quad (2)$$

where  $A_n$  and  $B_n$  are, respectively, the amplitudes of the incident and reflected waves in the  $n$ th layer,  $\alpha_n = \omega/c\sqrt{\varepsilon_n - \sin^2 \theta}$ , and  $\theta$  is the angle of incidence of the radiation. The magnetic field distribution in the layers is given by the expression

$$H_y(n, t) = [\sqrt{\varepsilon(n)} A_n e^{i\alpha_n(z-z_n)} - \sqrt{\varepsilon(n)} B_n e^{-i\alpha_n(z-z_n)}] e^{-i\omega t}. \quad (3)$$

From the continuity of the electric  $E_x$  and magnetic  $H_y$  fields at the interface  $z = z_{n-1}$  between the layers, we obtain the system of equations, which can be represented as the matrix equation

$$\begin{pmatrix} A_{n-1} \\ B_{n-1} \end{pmatrix} = T_{n-1,n} \begin{pmatrix} A_n \\ B_n \end{pmatrix}, \quad (4)$$

where

$$T_{n-1,n} = \frac{1}{2} \begin{pmatrix} (1+h)e^{-i\alpha_n\gamma_n} & (1-h)e^{i\alpha_n\gamma_n} \\ (1-h)e^{-i\alpha_n\gamma_n} & (1+h)e^{i\alpha_n\gamma_n} \end{pmatrix} \quad (5)$$

is the transfer-matrix. Here,  $h = \sqrt{\varepsilon_n - \sin^2 \theta}/\sqrt{\varepsilon_{n-1} - \sin^2 \theta}$  and  $\gamma_n = z_n - z_{n-1}$  (where  $n = 1, 2, \dots, N$ ) is the thickness of the  $n$ th layer. Equation (4) yields the following relation of the amplitudes of the waves that are incident on the resonant

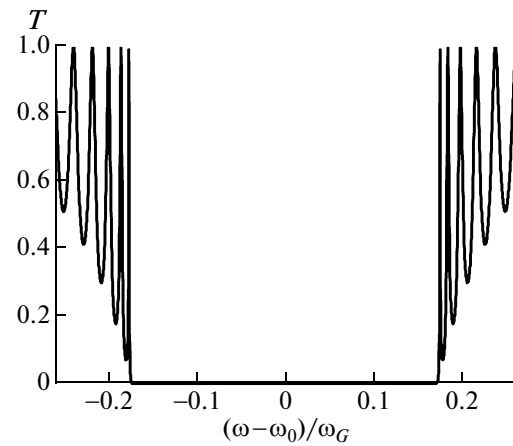


**Fig. 2.** Frequency dependences of transmission coefficient for *p*-polarized waves. Resonant photonic crystal considered consists of 30 periods, is 3  $\mu\text{m}$  thick, and has  $\varepsilon_1 = 3.0$  and  $\varepsilon_2 = 1.0$ .

photonic crystal and are reflected from it ( $A_0$  and  $B_0$ ) with the amplitude  $A_s$  of the wave emerged from the sample provided that the reflection of waves from the right-hand side of the resonant photonic crystal does not occur ( $B_s = 0$ ):

$$\begin{pmatrix} A_0 \\ B_0 \end{pmatrix} = \hat{M} \begin{pmatrix} A_s \\ 0 \end{pmatrix}, \quad (6)$$

where

$$\hat{M} = \hat{T}_{01} \hat{T}_{12} \dots \hat{T}_{N-1,N} \hat{T}_{N,S}, \quad (7)$$

$S = N + 1$ ,  $\gamma_{N+1} = 0$ . Finally, using (7), we obtain the transmission and reflection coefficients

$$T = 1/\left|\hat{M}_{11}\right|^2, \quad R = \left|\hat{M}_{11}\right|^2 / \left|\hat{M}_{21}\right|^2, \quad (8)$$

where  $\hat{M}_{11}$ ,  $\hat{M}_{21}$  are the elements of the matrix  $\hat{M}$ . The absorption coefficient is  $A = 1 - T - R$ .

## CALCULATION RESULTS

Let us now study particular features of the transmission spectrum of a resonant photonic crystal by numerically solving Eq. (8) for the transmission coefficient. The photonic crystals parameters chosen for these calculations were close to the following parameters used in [10]:  $\varepsilon_1 = 3.0$ ,  $d_1\sqrt{\varepsilon_1} = d_2\sqrt{\varepsilon_2}$ , the structure period is  $L = d_1 + d_2 = 100$  nm, and the number of periods is 30. Hg was taken as a resonant gas, for which  $\gamma/\omega_G = 1.65 \times 10^{-7}$  and  $\omega_p^2/\omega_G^2 = 7 \times 10^{-8}$ , where  $\omega_G = \pi c/L_0$  is the characteristic frequency of the bandgap and  $L_0 = d_1\sqrt{\varepsilon_1} + d_2\sqrt{\varepsilon_2}$  is the optical thickness. The width of the resonance line at  $\lambda_0 = 253.6$  nm is  $\gamma = 1.2 \times 10^9$  Hz.

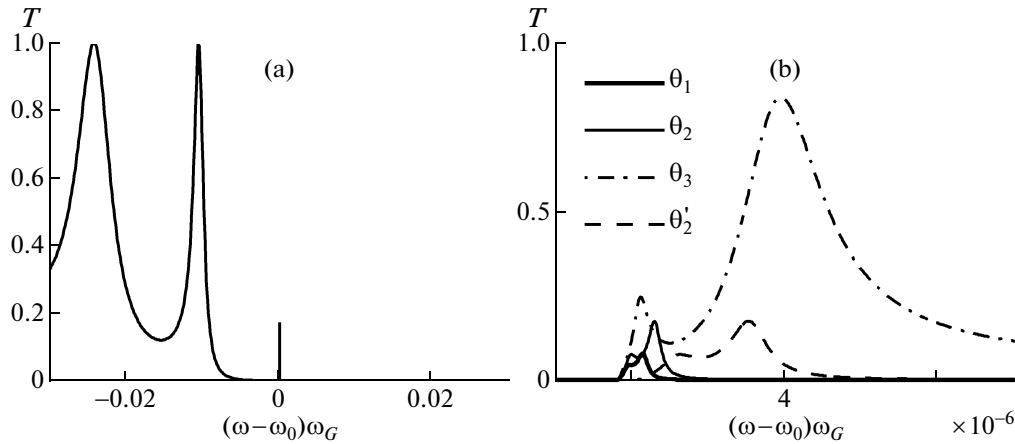


**Fig. 3.** Frequency dependence of additional transmission coefficient  $T$  in first bandgap of resonant photonic crystal. (a) Spectrum for  $p$ -polarized waves in vicinity of short-wavelength edge of bandgap with additional transmission peak and (b) structure of peaks. Angles of incidence are  $\theta_1 = 35^{\circ}12'$ ,  $\theta_2 = 35^{\circ}30'$ , and  $\theta_3 = 36^{\circ}12'$ ; density of resonant atoms is  $N = 4 \times 10^{14} \text{ cm}^{-3}$ ; and  $\gamma = 1.65 \times 10^{-7} \omega_G$ . Dashed curve is calculated for  $\theta'_2$  when  $N = 12 \times 10^{14} \text{ cm}^{-3}$  and  $\gamma = 4.95 \times 10^{-7} \omega_G$ . Dielectric permittivities are  $\epsilon_1 = 3.0$ ,  $\epsilon_2 = \epsilon_2(\omega)$ . Other parameters are the same as in Fig. 2.

Figure 2 shows a typical seed band structure of the transmission spectrum of a photonic crystal with  $\epsilon_1 = 3.0$  and  $\epsilon_2 = 1.0$  for  $p$ -polarized waves in the case of the normal incidence of radiation on the sample. The first bandgap of this photonic crystal lies in the wavelength region 215.8–307.4 nm, and the frequency  $\omega_0$  lies in the center of this region. Taking into account the frequency dispersion of the dielectric permittivity (1) leads to qualitative changes in the structure of the seed absorption spectrum.

Due to the combination of the dispersion of the photonic crystal structure with the resonant dispersion of the gas, an additional narrow transmission band

(which is indistinguishable on the scale of Fig. 2) appears in the bandgap of the photonic crystal. As an example, Fig. 3a shows the frequency dependence of the additional transmission coefficient of the resonant photonic crystal for the angle of incidence  $\theta_2 = 35^{\circ}30'$ . According to the Bragg condition, an increase in the angle of radiation incidence leads to a shift of the low-frequency edge of the bandgap to the resonance frequency  $\omega_0$  and to an increase in the transmission coefficient. As can be seen from Fig. 3b, the transmission coefficient is rather sensitive to a change in the angle  $\theta$  when the bandgap edge is close to  $\omega_0$ . An increase in the angle of incidence from  $35^{\circ}12'$  to  $36^{\circ}12'$ , i.e., by  $1^{\circ}$ , results in the 27-fold increase in the transmission coefficient, while the additional transmission band maximum reaches 83%. The full linewidth at half-maximum increases with increasing  $\theta$ . It is comparable with the resonance linewidth  $\gamma$  for  $\theta_2$  and is an order of magnitude larger for  $\theta_3$ . Note that the transmission at an angle  $36^{\circ}12'$  without taking into account the atomic gas dispersion ( $\epsilon_2 = 1.0$ ) is 3%.

As the density of the resonant gas is increased by a factor of three, the decay also increases threefold in the case of the impact broadening mechanism. The spectrum of the transmission band corresponding to  $\theta'_2$  (dashed curve in Fig. 3b) shifts from the resonance and the bandwidth increases threefold, while the transmission coefficient in the band peak does not change.

Figure 4 shows the refractive index and field intensity distributions in the sample for  $\theta = 35^{\circ}30'$ . The field frequency corresponds to the maximum transmission coefficient at the angle of incidence  $\theta = 35^{\circ}30'$ . As can be seen from Fig. 4, the field amplitude is maximum inside the sample and decreases to the

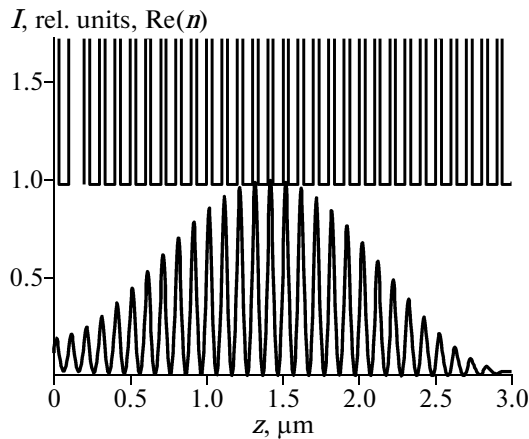


**Fig. 4.** Distribution of refractive index  $Re(n)$  over depth of resonant photonic crystal along  $z$  axis and same distribution of field intensity  $I$  normalized to its maximum value inside resonant photonic crystal. Field frequency corresponds to the transmission maximum at angle of incidence  $\theta_2 = 35^{\circ}30'$ . Other parameters are same as in Fig. 3.

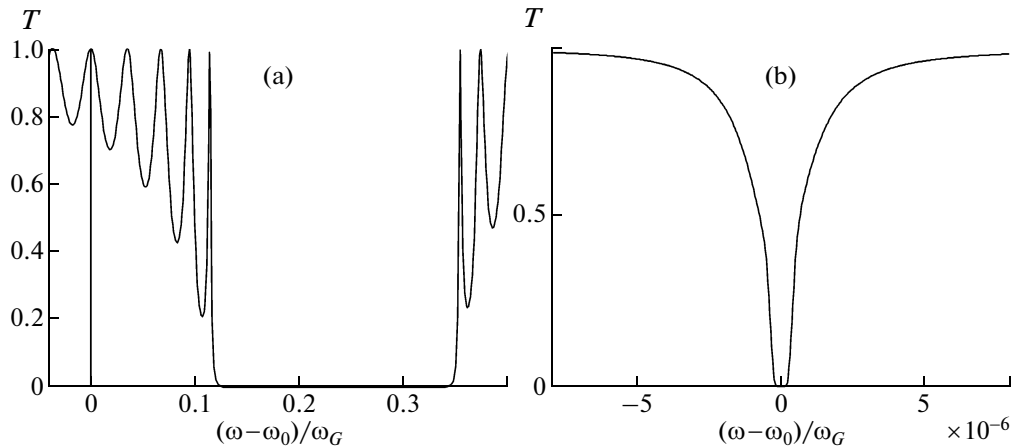


**Fig. 5.** Dependence of transmission coefficient of absorbing resonant photonic crystal on frequency detuning  $\omega$  from resonance frequency of gas  $\omega_0$ . (a) Additional bandgap in continuous spectrum at frequency  $\omega = \omega_0$ . (b) Transmission curve corresponding to the additional bandgap. Density of resonant atoms is  $N = 4 \times 10^{14} \text{ cm}^{-3}$ ,  $\gamma = 1.65 \times 10^{-7} \omega_G$ , and  $\theta = 45^\circ$ . Other parameters are same as in Fig. 3.

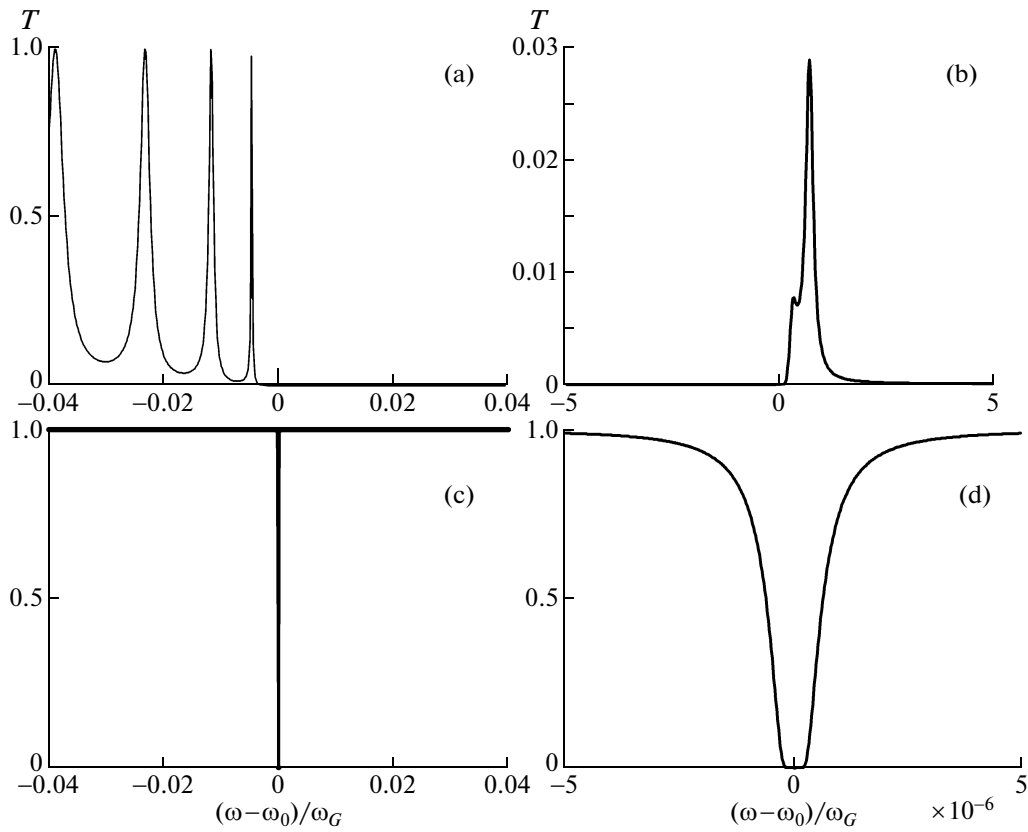


**Fig. 6.** Dependence of transmission coefficient of absorbing resonant photonic crystal on frequency detuning  $\omega$  from resonance frequency of gas for  $s$ - and  $p$ -polarized waves. (a) Spectrum near short-wavelength edge of bandgap with additional transmission peak at  $\omega = \omega_0$  and (b) the peak structure in the case of the  $s$  polarization. (c) Spectrum with single bandgap and (d) bandgap structure in case of  $p$ -polarized waves. Density of resonant atoms is  $N = 4 \times 10^{14} \text{ cm}^{-3}$ ,  $\gamma = 1.65 \times 10^{-7} \omega_G$ , and angle of incidence is  $\theta = \theta_B = 60^\circ$ . Other parameters are same as in Fig. 5.

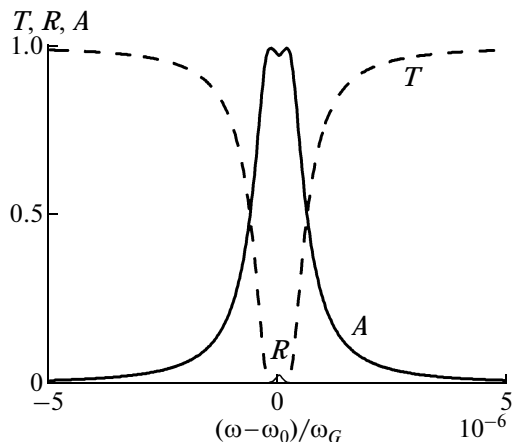


**Fig. 7.** Transmission  $T$ , reflection  $R$ , and absorption  $A$  coefficients for  $p$ -polarized waves as functions of frequency. Angle of incidence is  $\theta = 60^\circ$ ; other parameters are same as in Fig. 6.

right-hand of the interface between the resonant photonic crystal and vacuum. The electric field is almost completely localized in layers with high refractive indices.

For the resonant photonic crystal structure considered, there exists an angle of incidence at which the low-frequency edge of the bandgap shifts such that the resonance frequency falls into the continuous spectrum. In this case, the combination of the resonant dispersion of the gas with the dispersion of the photonic crystal structure results in the appearance of an additional bandgap in the transmission spectrum. This effect is illustrated in Fig. 5. The additional bandgap is shown for  $\theta = 45^\circ$ , at which the resonance frequency  $\omega_0$  coincides with the frequency of the fifth subsidiary maximum (Fig. 5a). The additional bandgap is rather narrow; as can be seen on the scale of Fig. 5b, its width is an order of magnitude larger than the resonance linewidth  $\gamma$ .

Note that the above-considered particular features of the transmission spectra of the resonance photonic crystal for  $p$ -polarized waves are also retained for waves with the  $s$  polarization. The bandgap for the  $p$ -polarized waves is reduced to zero at the angle of incidence equal to the Brewster angle  $\theta_B$ , since the Fresnel reflection at the interface in this case is absent and the transmission coefficient is  $T = 1$ . In our model for  $\epsilon_1 = 3.0$  and  $\epsilon_2 = 1.0$ ,  $\tan \theta_B = n_1 = \sqrt{3}$  and, hence, the Brewster angle is  $\theta_B = 60^\circ$ . Figure 6 shows the transmission spectra of the absorbing resonant photonic crystal for  $s$ - and  $p$ -polarized waves at the angle of incidence  $\theta = \theta_B$ . One can see that the structure of the transmission spectra is different for the  $s$ - and  $p$ -polarized waves. At the radiation frequency equal to the resonance frequency of the gas ( $\omega = \omega_0$ ), the transmission coefficients are zero, i.e., radiation of any polar-

ization cannot pass through the crystal. The transmission spectrum for  $s$ -polarized waves contains an additional low-intensity peak near the low-frequency edge of the bandgap at the frequency  $\omega \approx \omega_0$  (Fig. 6a). The structure of this peak is clearly seen in Fig. 6b. In the transmission spectrum for  $p$ -polarized waves (Fig. 6c), all bandgaps disappear except for one bandgap, whose width is an order of magnitude larger than the resonance linewidth  $\gamma$  (Fig. 6d). The frequency of the bandgap center almost coincides with the resonance frequency of the gas  $\omega_0$ .

Figure 7 presents the frequency dependences of the transmission (see Fig. 6d), reflection, and absorption coefficients of a resonant photonic crystal for  $p$ -polarized waves. It is seen that the bandgap in the transmission spectrum at the angle of incidence  $\theta = \theta_B$  is caused mainly by the absorption, which is maximum at  $\omega = \omega_0$ . The reflected wave is almost absent.

## CONCLUSIONS

The spectral properties of a one-dimensional structure filled with a resonant gas and having photonic bandgaps are calculated. The calculations showed that it is indeed possible to efficiently control the parameters of additional transmission in the bandgap of the resonant photonic crystal, as well as the parameters of additional bandgaps, by varying the resonant gas density and/or the angle of incidence of the light beam. Since a transmission band appears in the photonic bandgap, where radiation cannot propagate, it is possible to achieve filtration of optical radiation with a high contrast. It is also shown that the transmission spectra for  $s$ - and  $p$ -polarized waves at the angle of incidence equal to the Brewster angle of the seed photonic crystal are qualitatively different in the narrow frequency region near the resonance frequency of the gas. At the incident light frequency close to the resonance frequency of the gas, the transmitted light intensity decreases to zero. This creates additional possibilities for controlling the polarization and transmission of light. In addition, resonant photonic crystals can be promising for creation of spectral prisms with enhanced dispersion and narrowband filters with controlled characteristics needed to construct new types of optical devices.

## ACKNOWLEDGMENTS

This work was supported by grants NSh-7810.2010.3, RNP-2.1.1.3455; No. 27.1 and No 3.9.1 RAN, No. 5 and No. 144 SO RAN, and by the FTP “Scientific and Scientific-Pedagogical Personnel of Innovative Russia” (state contract no. 02.740.11.0220).

## REFERENCES

1. J. D. Joannopoulos, R. D. Meade, and J. N. Winn, *Photonic Crystals* (Princeton University Press, Princeton, 1995).
2. A. Yariv and P. Yeh, *Optical Waves in Crystals: Propagation and Control of Laser Radiation* (Wiley, New York, 1984; Mir, Moscow, 1987).
3. V. F. Shabanov, S. Ya. Vetrov, and A. V. Shabanov, *Optics of Real Photonic Crystals: Liquid-Crystal Defects and Inhomogeneities* (Sib. Otd. Ross. Akad. Nauk, Novosibirsk, 2005) [in Russian].
4. A. M. Zheltikov, Usp. Fiz. Nauk **170** (11), 1203 (2000).
5. O. Painter, R. Zec, A. Yariv, et al., Science **264**, 1819 (1999).
6. M. G. Martem'yanov, T. V. Dolgova, and A. A. Fedyanin, Zh. Éksp. Teor. Fiz. **125** (3), 527 (2004).
7. F. Wong, S. N. Zhu, K. F. Li, et al., Appl. Phys. Lett. **88**, 071102 (2006).
8. S. Ya. Vetrov, I. V. Timofeev, and A. V. Shabanov, Phys. Stat. Solidi (RRL) **1** (3), 92 (2007).
9. K. Busch, S. Lölkes, R. B. Wehrspohn, and H. Föll, *Photonic Crystals: Advances in Design, Fabrication, and Characterization* (Wiley-VCH, Weinheim, 2004).
10. A. M. Zheltikov, A. N. Naumov, P. Barker, and R. B. Maïls, Opt. Spektrosk. **89** (2), 309 (2000) [Opt. Spectrosc. **89** (2), 282 (2000)].
11. M. Rossa, G. Artoni, and F. Bassani, Phys. Rev. E **72**, 046604 (2005).
12. S. Ya. Vetrov, I. V. Timofeev, and A. Yu. Kutukova, Opt. Spektrosk. **106** (5), 840 (2009) [Opt. Spectrosc. **106** (5), 757 (2009)].
13. P. Yeh, J. Opt. Soc. Am. **69** (5), 742 (1979).

*Translated by M. Basieva*